

RESEARCH ARTICLE

Design of a Machine Learning Approach to Anomaly Detection in Tyre-Road Interaction

ALEKSANDR SAKHNEVYCH¹, NICOLA PASQUINO², (Senior Member, IEEE),
AND GIANCARLO SPERLI², (Member, IEEE)

¹Dipartimento di Ingegneria Industriale, Università degli Studi di Napoli Federico II, 80125 Napoli, Italy

²Dipartimento di Ingegneria Elettrica e delle Tecnologie dell'Informazione, Università degli Studi di Napoli Federico II, 80125 Napoli, Italy

Corresponding author: Giancarlo Sperli (giancarlo.sperli@unina.it)

ABSTRACT Tyres show a strong non-linear dependence on vertical force, road roughness, wear level, temperature gradient, and slip resulting in an additional challenge in calibration, whose parameters may vary significantly with the tyre's condition. An additional challenge to identifying and modeling the multi-dimensional tyre variability lies in the low accuracy level of tyre-road interaction data presenting physical inconsistencies and outliers, thus affecting outdoor testing scenarios. Indeed, outliers, gaps, or errors in the data can compromise calibration performance, potentially leading to incorrect model identification and rendering it unsuitable for further offline and online applications. In this paper, the authors aim to optimize the process of identifying tyre parameters by applying machine learning techniques to the dataset's pre-processing with particular attention to clustering and anomaly detection algorithms. The process is split into two phases: first, different clustering algorithms are applied to the tyre data to group similar operating conditions; then, anomaly detection algorithms are applied to clustered data to recognize and remove inconsistencies. Additionally, to objectively compare the proposed data processing results, the preprocessed specifically acquired experimental data have been employed for the calibration of the reference mathematical tyre formulation, comparing the deviations of the fundamental tyre-related quantities to the previously identified tyre model, already validated in both offline and online scenarios. For the grip coefficient evaluation versus both lateral and longitudinal slip variables, the Elliptic Envelope algorithm shows to be the best anomaly detection algorithm while the One-Class Support Vector Machine technique demonstrates lower deviations for the stiffness evaluation in both longitudinal and lateral directions.

INDEX TERMS Clustering, measurements, anomaly detection, nonlinear system calibration, outlier detection, tyre-road interaction.

I. INTRODUCTION

With the widespread application of Information and Communication Technology (ICT) starting from the earliest phases of the vehicle's design, the ability to reproduce the system's behavior in the widest possible range of conditions of interest has become crucial for the reduction of development time, costs and risks [1], [2]. The heterogeneous environment and harsh operating conditions of tyres frequently introduce instability and unreliability into their performance [3]. Moreover, the ability to evaluate system parameters using

real-time signals enables necessary improvements in control systems and advances future smart mobility, considering not only vehicle performance and safety but also overall grid efficiency and environmental impact [4], [5]. In this scenario, autonomous vehicles should become increasingly able to preserve their maneuverability in a wider range of driving conditions and environmental adversities, assuring that the system's state and run-time parameters are estimated with good accuracy [6], [7], [8].

Initially, anomaly detection methods were employed in fields such as cybersecurity and finance, later extending to vehicle dynamics, where early techniques relied on statistical models and signal processing to identify anomalies in

The associate editor coordinating the review of this manuscript and approving it for publication was Mohammad J. Abdel-Rahman¹.

sensor data like tyre pressure, vehicle accelerations or road conditions [9], [10]. To this purpose, unsupervised machine learning (ML) techniques such as autoencoders and K-means can be applied to analyze complex tyre dynamics [11], [12], facilitating the detection of subtle deviations in tyre behavior, especially for evaluating adherence coefficient [13]. Furthermore, the rise of deep learning brought Recurrent Neural Networks (RNNs) and Convolutional Neural Networks (CNNs) into the field, which can allow real-time analysis of more complex data from state observers and physical sensors, and improve the detection of patterns related to friction loss [14], [15] although the noise and dynamic environment poses several challenges in the train and inference process of deep learning-based models [16].

Recent technological advancements, including connected vehicles and the use of advanced tyre sensors [17], [18], have further enhanced anomaly detection [19]. Integrating data like weather conditions and road surfaces has boosted predictive capabilities, helping identify potential issues before they occur. Looking ahead, the continued evolution of ML, coupled with autonomous systems, could lead to vehicles capable of self-diagnosing and preventing tyre grip loss, thereby significantly improving vehicle performance and road safety [20], [21].

From a global perspective, the current state of ML approaches to anomaly detection exhibits significant challenges, particularly in unexplored domains like tyre modeling: data representativeness with restricted generalization capabilities [22], [23]; real-time computational constraints struggling with high computational overhead and multi-dimensional sensor data [24], [25]; black-box ML techniques predominantly used in anomaly detection lack transparent decision-making processes [26]; validation limitations with inconsistent evaluation metrics and restricted experimental environments [27], [28]. The studies available in the literature about the application of ML to anomaly detection for vehicle dynamics mainly concern real-time and edge-based applications [29]. This is an important area, especially given the complexities of increasingly automated driving systems, which integrate multiple sensing technologies, real-time processing of large and heterogeneous sensor data under strict energy consumption constraints, and the need for robust safety and security measures [30], [31]. On the other hand, the current study leverages ML techniques not for direct real-time anomaly detection as intended in the literature, but to explore their potential in improving the estimation of key parameters related to tyre-road interaction, such as tangential forces and corresponding slips [32], [33]. Indeed, the primary aim of this work is to evaluate whether ML algorithms can enhance the identification of critical parameters of interest like stiffness and grip, using raw acquired data [34], [35].

In this context, a major challenge regards the calibration of non-linear systems, whose parameters may vary significantly with the system's state [36]. In the case of a vehicle, tyres show a strong non-linear dependence on factors like

vertical force, road roughness, wear level, temperature gradient, and slips [37]. However, an additional challenge to identifying and modeling the multi-dimensional variability lies in the poor accuracy of the tyre-road interaction data when physical inconsistencies and outliers are present, thus affecting outdoor testing scenarios [35], [38]. Indeed, the presence of outliers, gaps, or errors in the dataset could potentially jeopardize the calibration performance, leading to model misidentification and the consequent unsuitability for further applications concerning both offline and online applications [34], [39], [40]. Once the testing methodology and a specific set of sensors have been chosen, the goal is to explore the tyre behavior in the widest possible operating conditions to ensure a sufficiently representative dataset for model calibration. Indeed, due to the intrinsic non-linearity and the amount of additional multi-physical quantities to be accounted for, the accuracy and robustness of the model calibration are directly linked to the degree of completeness and quality of acquired data.

Regarding vehicle dynamics, some approaches in the literature rely on a model-based framework employing Gaussian Process Regression to predict tyre properties [41] or lateral forces [42]. Nevertheless, the complexity in modeling non-linear and dynamic systems like tyre-road interaction and the sensitivity of tyres to parameters strongly affect the effectiveness of such approaches. As tyre-road interaction estimation is a significant challenge in the literature as underlined in [3], researchers have designed ML models based on acceleration data to classify tyre tread wear [43] and performances prediction [44], or to approximate nonlinear tyre model for predictive control [45]. Nevertheless, the non-linear behavior and measurement uncertainty affect the effectiveness of the state-of-the-art approaches, demanding more and more complex pre-processing strategies. To deal with this complexity, the authors propose an unsupervised approach to provide the essential data for an accurate tyre's model calibration process. Hence, the authors propose a data-driven-based pipeline, in which cluster algorithms are firstly applied to group samples with similar behaviors, and then anomaly detection algorithms are used to unveil anomalous behaviors of tyres.

For both indoor and outdoor experimental data, it is necessary to define an outlier as an anomalous value within a set of observations for the same input. However, scientifically establishing a robust index is not trivial, especially when the number of available samples is low. Moreover, in single-variable observations, an outlier is a sample with a surprisingly low or high value, while in multivariate datasets, unexpected factors may arise from interrelationships between variables.

To this purpose, the authors investigate the application of established clustering algorithms (K-Means, K-Medoids, Gaussian Mixture Models, and Hierarchical Clustering) to the chosen reference model to identify similar force conditions in the tyre-road contact plane. The resulting clusters are

analyzed on tyre behavior curves using anomaly detection techniques i.e., One-Class Support Vector Machine (SVM) (OC-SVM), Isolation Forest (IF), Local Outlier Factor (LOF), and Elliptic Envelope (EE)), followed by a physical evaluation assessing characteristic points' proximity to a reference curve. Rather than proposing new methodologies, this work focuses on systematically applying and evaluating existing clustering and anomaly detection techniques, extensively analyzing and benchmarking, to formulate the most effective approach for the specific domain of tyre-road interaction anomaly detection.

Summarizing, the proposed analysis is mainly synthesized in the following steps:

- different clustering algorithms (i.e., *K-Means*, *K-Medoids*, *Gaussian Mixture Models* and *Hierarchical models*) are fed as inputs to the Pacejka's tyre model for identifying similar kinematic-dynamic conditions arising in the tyre-road contact area;
- different anomaly detection algorithms (i.e., OC-SVM, IF, LOF, EE) are applied on top of the clustered data to remove the undesired non-physical outliers;
- proposed approaches are benchmarked using a real-world dataset, composed of measurements collected through an experimental campaign using a FIAT 124 RWD Spider vehicle mounting Toyo Porxes R888R 196/50R16 at the Sele track, Italy.

The paper is organized as follows: in Section II a typical problem regarding the necessity to heavily pre-process the acquired tyre data is presented, investigating the causes and proposing the solutions available in literature and industry. In Section III-B, following the data cleaning and normalization phases, different clustering algorithms are applied to tyre data to group observations into different clusters to optimize the model identification process. Section IV describes the experimental campaign, reporting the vehicle parameters and the main characteristics of the sensing equipment employed. Section V presents the outcomes of the presented anomaly detection algorithms applied to each data cluster, discussing their benefits and comparing the identification accuracy of the tyre-road interaction main quantities like stiffness and maximum friction versus the ones of an already validated tyre digital twin obtained by the authors for the same tyres in previous work.

II. PROBLEM DEFINITION

The tyre data containing the required kinematic and dynamic observations of the main variables of interest (i.e., thermodynamics, wear, pavement characteristics) are commonly collected in indoor and outdoor scenarios. The experimental protocol includes acquiring data employing both indoor test rigs (e.g., drum [46], [47] or flat belt [48], [49]) and outdoor sessions, considering the vehicle as a moving lab [38], [50] or a dedicated trailer.

Indoor testing is preferred for its intrinsically controlled and sensorized environment, where the deeply

inter-connected phenomena of the tyre behavior can be decoupled thanks to the quality and accuracy of the acquired signals and the possibility of designing the testing routine according to the specific characterization purpose [51], [52]. The tyre typically spins in contact with a drum or a rolling belt covered with steel or abrasive paper. At the same time, different load and kinematic conditions are applied and the resulting interaction forces and torques are measured. However, indoor test procedures have several inherent limitations. Firstly, the friction coefficient is evaluated by imposing unstable operating conditions on the tyre, which can be challenging to control due to the vibrations of the belt-rim system, leading to an overestimation of the adhesion coefficient. Secondly, tyres are not tested under real working conditions, which are hard to reproduce in a laboratory environment, since the belt roughness parameters differ significantly from the real asphalt characteristics.

Gathering tyre data in real-world scenarios requires outdoor testing, where the tyre faces dynamic conditions by engaging with diverse road surfaces and environmental scenarios [32]. Several methodologies, making use of Inertial Measurement Units (IMUs), Global Positioning System (GPS), sideslip sensors, wheel force transducers, encoders, and sophisticated moving benches have been developed for outdoor testing [33], [53], [54], [55]. With this aim, several vehicle dynamic models [38], [56], confidential procedures [57], model-based filters [58], and advanced moving lab-trailers [32], [59] have been designed to explore all possible tyre operating conditions also in outdoor testing [60]. A key advantage is the ability to directly capture the complex, nonlinear behaviors of tyre-road interactions specific to certain pavement textures. Outdoor testing, in particular, yields more realistic and reliable data, making it invaluable for tyre modeling and simulation. However, outdoor testing also has some disadvantages, such as the challenge of controlling and measuring test variables, the high cost and time required for the experiments, and the safety issues related to the testing personnel and equipment, with a specific focus on ensuring the quality and repeatability of the results. In addition, in this context, it is often challenging to ensure that the tyre operates near its limit conditions, which is particularly valuable for calibration purposes. This is especially relevant for parameters like the maximum friction coefficient, or the forces and torques under pure conditions at high slip angles [32], [61].

Be it an indoor or outdoor scenario, the minimum necessary dataset consists of kinematic and dynamic data, to represent the tyre-road interaction curves in the widest range of tyre operating conditions, in terms of vertical load, inflation pressure, slip angle, slip ratio, and inclination angle [32], [62]. Advanced and more recent studies also consider the road surface characteristics and the compound viscoelastic properties, as well as temperature and wear states, among the multidimensional independent variables to account for to investigate and to model the tyre behavior [35], [63]. Among the quantities to measure, a particular effort

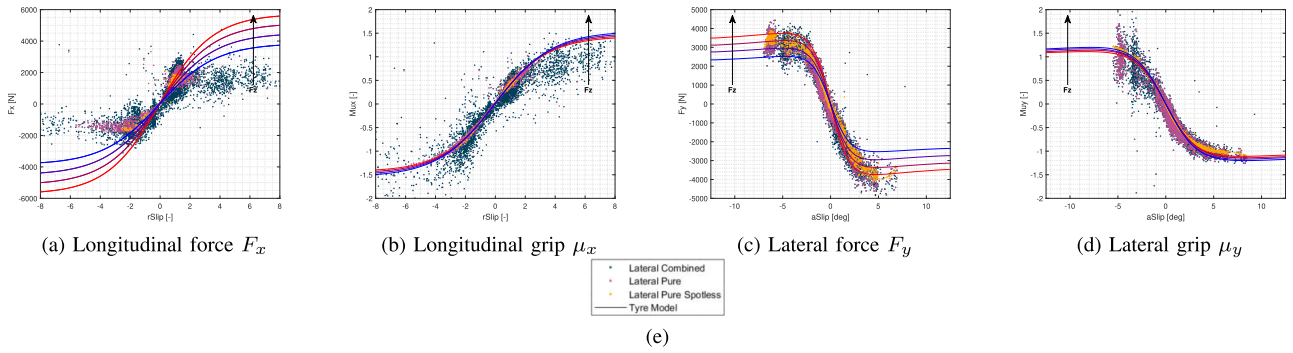


FIGURE 1. Tyre-road interaction data analysis and modeling.

lies in evaluating the tyre kinematics, since the only sensors usually available consist of the wheel encoder to measure the tyre’s angular velocity and a wire sensor to assess the steering angle. The longitudinal and lateral slips, s_r (or $rSlip$) and s_a (or $aSlip$) respectively, are defined as:

$$\begin{aligned} s_r &= \frac{v_x - \omega R_{\text{eff}}}{|v_x|}, \\ s_a &= \arctan \frac{v_y}{|v_x|}. \end{aligned} \quad (1)$$

where R_{eff} is the tyre rolling radius, ω is the wheel angular velocity, and v_x and v_y are the longitudinal and lateral velocities of the tyre’s contact patch velocity. When it comes to indoor testing, the above quantities can be measured and parameterized with a reasonably high degree of accuracy [51], [52]. In outdoor testing scenarios, the velocity components of the wheel are typically measured using dedicated sensors, such as optical [64] or IMU-based [64] devices. These measurements are then kinematically transformed to the point of interest, usually the wheel’s hub [38], while the wheel’s angular velocity is obtained using specialized OEM encoders [65]. Additionally, knowledge of the instantaneous wheel alignment, the equivalent normal direction at the road contact patch, and the rolling radius form the basis for evaluating tyre slips. Unfortunately, due to various factors such as road conditions, tyre thermodynamic and wear states, steering and suspension systems’ compliance, and environmental variations, analyzing tyre slip during outdoor testing can lead to significant inaccuracies [33], [54].

It is worth to note from Figure 1 that data pre-processing is an essential step in building a reliable and accurate model. One of the main tasks of data pre-processing is to detect and remove outliers, which are data points that deviate significantly from the rest of the data. Outliers can have a negative impact on the model performance, as they can introduce noise, bias, and distortion. Therefore, it is important to apply appropriate methods for outlier detection and removal before feeding the data to the model. This way, the model can learn from a clean and representative data set, and achieve better robustness and accuracy.

Among the tyre formulations, to physically transform the kinematic signals in dynamic data, Pacejka’s Magic Formula (MF) model has been preferred as it offers a remarkable compromise between accuracy and robustness in real tyre representation and quite low computational effort, which makes it particularly suitable for both real-time driving simulations and for offline performance optimization algorithms.

The analytical expression of the MF mathematical model has been defined according to [35], [66]:

$$y(x) = D \cdot \sin \left[C \cdot \arctan \left\{ B \cdot x - E \cdot (B \cdot x - \arctan(B \cdot x)) \right\} \right] \quad (2)$$

with

$$\begin{aligned} Y(x) &= y(x) + S_v, \\ x &= X + S_h \end{aligned} \quad (3)$$

where $Y(x)$ is a dynamic output (F_x , F_y or M_z), X is the kinematic input (slip ratio s_r or slip angle s_a defined in Equation (1)), B is the rigidity factor, C is the shape factor, D is the peak value, E is the bending factor, S_v and S_h are the vertical and horizontal shifts, respectively.

The above six quantities are the MF macro-coefficients, defining Pacejka’s curve shape. Each macro-coefficient is itself a polynomial (linear, quadratic, trigonometric, exponential) function of the tyre’s kinematic and dynamic variables, combining several micro-parameters without a clear physical meaning (Figure 2a). Equation (2) describes only the pure conditions, which can be extended to the combined ones, introducing the “hill function” G defined in Equation (4) and represented in Figure 2b) [35], [66]:

$$G = \frac{\cos \left(C \cdot \arctan(B \cdot x - E \cdot (B \cdot x - \arctan(B \cdot x))) \right)}{\cos \left(C \cdot \arctan(B \cdot S_{h,x} - E \cdot (B \cdot S_{h,x} - \arctan(B \cdot S_{h,x}))) \right)} \quad (4)$$

III. PROCESSING METHODOLOGY

The proposed methodology shown in Figure 3 aims to optimize tyre’s parameter identification by using machine learning approaches, focusing on two phases: clustering

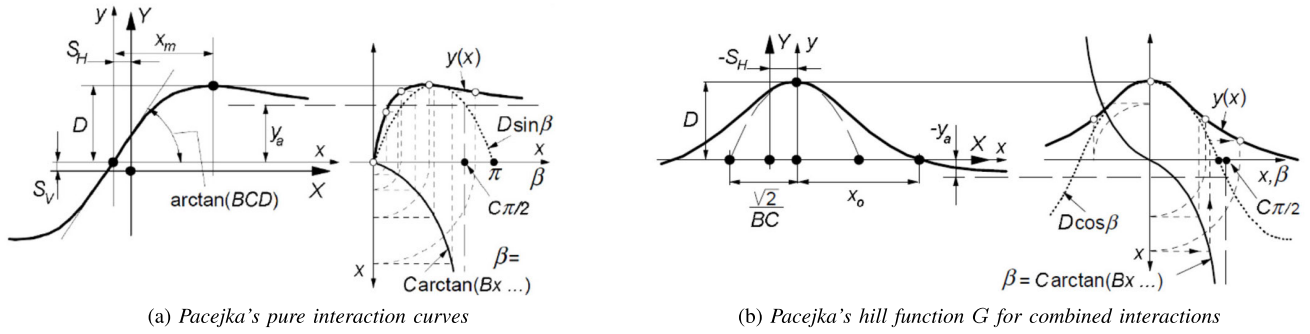


FIGURE 2. Pacejka's Magic Formula tyre model [66].

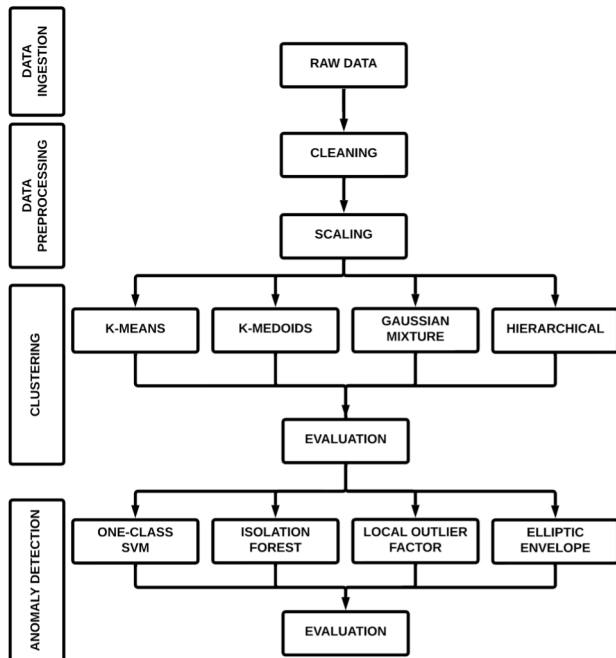


FIGURE 3. End-to-end methodology composed of four steps. After the acquisition, data undergo cleaning and standardization operations before clustering observations into homogeneous groups. Finally, several algorithms are applied to unveil anomalies in each cluster.

algorithms group similar operating conditions, followed by anomaly detection to eliminate inconsistencies within the clustered data. After performing a series of pre-processing operations (i.e., cleaning and standardization), different clustering algorithms are applied to tyre data to group similar observations into separate sets, which will later be investigated to estimate the tyre's parameters.

A. DATA INGESTION

For most car and tyre manufacturers, an instrumented vehicle is a more commonly used testing tool than test trailers. This preference is driven by the lower cost of utilizing commercially available vehicles fitted with sensors and instruments, which can be modified as required. This approach was chosen primarily for its cost-effectiveness, despite the understanding

that, even when properly employed, it offers lower setup accuracy than trailer testing.

B. DATA PRE-PROCESSING

Measurement data can be incomplete, duplicated, or out of range, therefore they need to be pre-processed to make them suitable for the analysis. After removing duplicated data, missing values are imputed through linear interpolation, and each feature is standardized [67] so that all of them have the same numerical scale and ensure that each one is weighted equally by the clustering algorithm.

C. CLUSTERING

In this section, we describe our clustering strategy aims to group samples with similar behaviors. A cluster analysis is performed to group similar observations of the input variables so that detection and labeling of anomalies in the output variables can be executed on homogeneous sets of observations for the subsequent tyre model identification. The authors have chosen four clustering algorithms based on the classification provided in [68]: K-Means and K-Medoids [69], and Gaussian Mixture [70], belonging to the *partitional* class; Agglomerative Hierarchical algorithm [71] representing the *hierachical* class.

D. ANOMALY DETECTION

In the past decade, the pervasive integration of ICT in several industrial environments has made it possible to harvest a large amount of data, whose processing can support a variety of tasks [72]. Furthermore, data quality can strongly affect the effectiveness of approaches [73], leading researchers and practitioners to focus on designing approaches for anomaly detection [74], which is an unsupervised learning task aiming to detect anomalous behavior in historical data [75], most times showing as outlier observations. As shown in [76], outliers in time series can have two different meanings: 1) they can be related to noise, erroneous, or unwanted data, which are not interesting to the analyst; 2) they represent unusual but interesting phenomena which are useful to detect and study. To identify anomalies, the authors have used four

unsupervised algorithms, that represent the most widely used, as underlined in [77], [78]:

- **One-Class Support Vector Machine (OC-SVM).** The OC-SVM [79], [80] anomaly detection algorithm relies on SVM, a classification algorithm that aims to maximize the *margin* [81], defined as the distance between the separation hyperplane (decision boundary) and the training samples closest to the hyperplane, named *support vectors*. Once the best hyperplane separating the two classes has been identified, observations are reprocessed with a sign function that labels the observations as +1 or -1 depending on where they are relative to the hyperplane, separating the normal from the anomalous values. Under unsupervised setting, the algorithm groups observations near the origin into one class, while assigning the remaining observations to a different class. One of the main reasons why the SVM is widely used is that you can use the *kernel trick* based on the radial-basis function for observations that are not linearly separable: those data can be separated by transforming features into a higher-dimensional space using the *kernel* which is easier and faster than a mapping function. In this way, data will be linearly separable through a hyperplane in the new space.
- **Isolation Forest (IF).** The IF [82], [83] relies on the idea that anomalies are *few and different* and, therefore, they are more susceptible to isolation than normal observations. A tree structure can help isolate each observation more effectively. Anomalies will be in the leaf nodes closest to the root node of the tree due to their susceptibility to isolation, while normal observations will be isolated in the leaf nodes farthest from the root node. The procedure through which the algorithm isolates anomalies starts by building binary isolation trees (*iTree*) to partition all the elements of the dataset. Partitions are generated by selecting a random feature of the dataset and a random value between the minimum and maximum of the feature. Hence, isolating a normal observation is more challenging and requires more partitions compared to isolating an anomalous point. To improve the quality of the algorithm, a forest of binary trees is created. Once the entire dataset is partitioned, the observations are reviewed within the forest, and an *anomaly score*, normalized to the number and depth of trees, is used to label observations as normal or anomalous.
- **Local Outlier Factor (LOF).** The LOF [84] evaluates the local density around each observation and compares it with the local density of its nearest neighbors. A point with a significantly lower local density than its neighbors will have a higher LOF value, which makes that observation a possible anomaly. Given a point, the algorithm computes its distance to the k nearest neighbors, which is subsequently used to determine its local reachability distance. Next, the local

reachability density is calculated as the inverse of the local reachability distance, and then the LOF score is calculated. If the score is less than 1, the observation has a higher density than neighbors and can be considered normal; if the score is greater than 1, the observation can be considered as an anomalous value.

- **Elliptic Envelope (EE).** The EE [85], [86] models data through an elliptic distribution, labeling all elements that fall outside the ellipsoid as anomalies. The algorithm has two steps: in the first one, it tries to find the best fit of a multivariate ellipsoid to the data, optimizing the center of the ellipsoid and the covariance matrix so that the sum of the quadratic errors between the dataset points and the ellipsoid itself is minimized. In the second one, observations are evaluated according to their distance to the ellipsoid, and elements falling outside the ellipsoid are considered anomalies.

IV. EXPERIMENTAL ANALYSIS

In this section, the experimental protocol designed to evaluate the presented data pre-processing approach is presented. Specifically, first a discussion of the experimental dataset characteristics is introduced in Section IV-A, then the measures of validity and error metrics are illustrated in Section IV-B, which are then adopted in Section IV-C to evaluate the identification results regarding the tyre model parameters.

A. DATASET

The experimental campaign was conducted on the Battipaglia circuit, in the context of SeaSide Racing 2023, in dry conditions with boundary 22 °C and 25 °C for air and track temperatures, respectively. A fully equipped FIAT 124 RWD Spider mounting Toyo Proxes R888R 195/50R16, which had been tested in indoor conditions beforehand, was employed as the testing vehicle to acquire the data samples required to reconstruct the tyre-road interaction curves represented in Fig. 1. The key vehicle's features are listed in Table 1.

The vehicle was equipped with advanced sensors to measure acceleration, velocity, force, and tyre temperature. The measurement systems and individual sensors of greatest interest were a dynamometer hub, a non-contact vehicle speed sensor, and an onboard computer to guarantee the correct functioning of all the devices and the consistency of all the collected experimental data. The complete measurement setup is reported in Table 2, also providing sensors' accuracy specifications.

Telemetry data were processed in Matlab as described in [38] to return the quantities of interest for each tyre: slip angle s_a , slip ratio s_r , camber angle γ , vertical force F_z , longitudinal force F_x and lateral force F_y . Lateral $\mu_y = F_y/F_z$ and longitudinal $\mu_x = F_x/F_z$ grip values were also calculated.

Missing (NaN) and infinite values occasionally encountered in the dataset due to sensing and logging singularities,

TABLE 1. Main characteristics of the vehicle.

| Parameter | Value |
|---------------------|---------------------|
| Vehicle mass | 1197.5 kg |
| Unsprung mass | 200 kg |
| Wheelbase | 2.31 m |
| CG x-position | 1.088 m |
| Front track | 1.495 m |
| Rear track | 1.505 m |
| CG z-position | 0.489 m |
| Vehicle inertia Izz | 950 km ² |
| Vehicle inertia Ixx | 730 km ² |
| Section area | 2.13 m ² |
| Front stiffness | 43.347 24 N/mm |
| Rear stiffness | 20.097 363 6 N/mm |
| Nominal steer ratio | 14.2 |
| Front static camber | 0.3° |
| Rear static camber | 0° |

TABLE 2. Acquired signals and sensors' accuracy specifications.

| Signal | Device | Accuracy/Sensitivity |
|---------------------------|-----------------------------------|---|
| Longitudinal velocity | S-Motion | < ±0.2% Range: up to 400 km/h |
| Lateral velocity | S-Motion | < ±0.2% Range: up to 400 km/h |
| Longitudinal acceleration | OxTS 3000 | Bias stability: 2 μg Range: ±10g |
| Lateral acceleration | OxTS 3000 | Bias stability: 2 μg Range: ±10g |
| Vertical acceleration | OxTS 3000 | Bias stability: 2 μg Range: ±10g |
| Yaw rate | OxTS 3000 | Bias stability: 2 °/h Range: ±100°/s |
| Steer angle | Angle Sensor (vehicle CAN-bus) | Resolution: 0.1° Range: ±780° |
| Wheel speed | Encoder (vehicle CAN-bus) | Timing accuracy: 2% Range: 0 Hz to 2500 Hz |

were identified and imputed by linear interpolation of the two closest values to guarantee the time continuity of all data channels of interest, directly measured and estimated, respectively. Those values were considered as anomalies in the following steps. Finally, as requested by clustering, each input variable x_i was standardized to z_i , according to Equation (5):

$$z_i = \frac{x_i - \bar{x}_i}{s_i}, \tag{5}$$

where \bar{x} and s_i are the sample mean and standard deviation, respectively.

Furthermore, the four clustering algorithms were applied to data from each tyre to unveil similar behaviors in terms of the tangential force on which anomaly detection algorithms have been applied to identify samples that differ from the normal ones.

B. MEASURES OF VALIDITY AND ERROR METRICS

To assess the effectiveness of the anomaly detection, several indices [87], [88] including the Elbow Curve, the Silhouette score, the Calinski-Harabasz, the Davies Bouldin, the Dunn, the C-Index, and the Akaike Information Criterion (AIC) and Bayesian Information Criterion (BIC) are adopted.

- **Elbow Curve.** The Elbow Curve [89] is a commonly used visual method for determining the optimal number of clusters in clustering algorithms, particularly in k -means clustering. The method is based on plotting a metric called *inertia*, which measures how tightly the data points are grouped within each cluster. Hence, inertia measures the compactness of the clusters—the lower the inertia, the closer the data points are to their respective centroids. Specifically, inertia is defined as the sum of squared distances between each data point and the centroid of its respective cluster. Mathematically, inertia is represented according to Equation 6:

$$\text{inertia} = \sum_{i=1}^n \sum_{j=1}^k \mathbb{I}(x_i \in C_j) \cdot \|x_i - c_j\|^2 \tag{6}$$

where: n is the number of data points, k is the number of clusters, C_j is the set of points in cluster j , x_i represents a data point, c_j is the centroid of cluster j , \mathbb{I} is an indicator function that equals 1 when x_i belongs to cluster C_j and 0 otherwise.

The Elbow Curve plots inertia on the y-axis against the number of clusters (k) on the x-axis. As the number of clusters increases, inertia decreases because the data points are partitioned into smaller, more localized groups. However, after a certain number of clusters, the rate of decrease in inertia slows down significantly. This point, known as the *elbow point*, represents a balance between reducing inertia and avoiding excessive complexity (i.e., having too many clusters). The elbow point is considered the optimal number of clusters, beyond which additional clusters provide diminishing returns in terms of improved clustering quality.

- **Silhouette score.** The Silhouette score [90] is a widely used metric for evaluating the quality of a clustering solution by measuring how similar an object is to its cluster compared to other clusters. It provides a comprehensive evaluation of both *cohesion* (how closely related points in the same cluster are) and *separation* (how well clusters are distinguished from each other). The Silhouette score for each data point is calculated according to Equation (7):

$$S(i) = \frac{b(i) - a(i)}{\max(a(i), b(i))} \tag{7}$$

where: $S(i)$ is the Silhouette score for data point i , $a(i)$ is the average distance between i and all other points in the same cluster (within-cluster cohesion), $b(i)$ is the lowest average distance between i and points in any

other cluster, which is the nearest neighboring cluster (between-cluster separation).

The Silhouette score ranges from -1 to 1 :

- a score close to 1 indicates that the data point is well clustered, with its cluster being highly compact and well-separated from other clusters.
- a score around 0 suggests that the data point lies near a cluster boundary, making it difficult to assign definitively to one cluster.
- a score close to -1 indicates that the data point might have been assigned to the wrong cluster, as it is closer to a different cluster than to its own.

The overall Silhouette score for a clustering solution is the average of the individual scores for all data points. A higher average Silhouette Score indicates better-defined, well-separated clusters.

- **Calinski-Harabasz index.** The Calinski-Harabasz index (also known as the Variance Ratio Criterion) [91] is a widely metric for evaluating the effectiveness and quality of clustering outcomes. It evaluates the ratio of the sum of between-cluster dispersion to within-cluster dispersion, offering insight into how well the clusters are separated and compact. A higher Calinski-Harabasz score indicates more distinct and well-separated clusters, signifying better clustering performance.

The formula for the Calinski-Harabasz index is given in Equation (8):

$$\text{CH Index} = \frac{\text{tr}(B_k)/(k-1)}{\text{tr}(W_k)/(n-k)} \quad (8)$$

where: $\text{tr}(B_k)$ is the trace of the between-cluster dispersion matrix, $\text{tr}(W_k)$ is the trace of the within-cluster dispersion matrix, n is the number of data points, k is the number of clusters.

The index evaluates clustering quality by balancing intra-cluster variance, which measures compactness within clusters, and inter-cluster variance, which assesses separation between clusters. Higher values means more distinct and well-defined clustering structures.

- **Davies-Bouldin index.** The Davies-Bouldin index [92] is a clustering evaluation metric that measures the quality of a clustering solution by examining both the compactness of clusters and the degree of separation between them. It is designed to assess how well the clusters are formed and separated from each other. A lower Davies-Bouldin index value indicates better clustering performance, where the clusters are more compact and better separated.

The Davies-Bouldin index is computed using the Equation (9):

$$\text{DB Index} = \frac{1}{k} \sum_{i=1}^k \max_{j \neq i} \left(\frac{s_i + s_j}{d_{ij}} \right) \quad (9)$$

where: k is the number of clusters, s_i is the average distance between each point in cluster i and the centroid of that cluster (a measure of intra-cluster dispersion or compactness), d_{ij} is the distance between the centroids of cluster i and cluster j (a measure of inter-cluster separation).

For each cluster i , the index calculates the similarity between cluster i and the cluster j that is most similar to it (in terms of a combination of compactness and separation). The overall Davies-Bouldin index is the average of these “worst-case” similarity scores across all clusters.

The main goal of the Davies-Bouldin index is to minimize the intra-cluster distances (making clusters more compact) and maximize the inter-cluster distances (ensuring well-separated clusters). Lower values of the index indicate that the clusters are dense and far apart, implying better clustering performance.

- **Dunn index.** The Dunn index [93] is a clustering evaluation metric that aims to identify clustering solutions where the clusters are well separated and internally compact. It evaluates both the intra-cluster compactness and inter-cluster separation, rewarding clustering solutions where the distance between clusters is large, and the points within clusters are closely packed.

The Dunn index is defined according to Equation (10):

$$\text{D Index} = \frac{\min_{1 \leq i < j \leq k} \delta(C_i, C_j)}{\max_{1 \leq l \leq k} \Delta(C_l)} \quad (10)$$

where: k is the number of clusters, $\delta(C_i, C_j)$ is the distance between the two most similar clusters C_i and C_j (inter-cluster separation), $\Delta(C_l)$ is the maximum intra-cluster distance in cluster C_l , which measures the compactness of the cluster.

The numerator $\delta(C_i, C_j)$ represents the smallest distance between two clusters (i.e., the minimum distance between any two clusters, encouraging larger inter-cluster separation), while the denominator $\Delta(C_l)$ captures the largest intra-cluster distance (i.e., the size of the least compact cluster). A higher Dunn index value indicates better clustering, where clusters are far apart and points within each cluster are tightly grouped.

The Dunn index is particularly useful for detecting well-separated, compact clusters and is sensitive to outliers. Higher Dunn index values reflect better clustering performance, meaning that both the separation between clusters and the compactness within clusters are optimized.

- **C-Index.** The C-Index [94] is a clustering evaluation metric that measures the quality of a clustering solution by comparing the total intra-cluster distances with the best and worst possible total intra-cluster distances for the given dataset. It assesses how well the clustering solution minimizes the distance between objects within the same cluster.

The C-Index is defined according to Equation (11):

$$C = \frac{\sum_{i=1}^n d(i) - S_{\min}}{S_{\max} - S_{\min}} \quad (11)$$

where: n is the number of intra-cluster pairs (pairs of points within the same cluster), $d(i)$ is the distance between each pair of points within the same cluster, S_{\min} is the sum of the distances for the n smallest pairwise distances in the entire dataset (representing the best-case clustering, where all closest points are in the same cluster), S_{\max} is the sum of the distances for the n largest pairwise distances in the entire dataset (representing the worst-case clustering, where the most distant points are in the same cluster).

The C-Index ranges from 0 to 1:

- A value close to 0 indicates that the intra-cluster distances are near the minimum possible, meaning that the clustering is well compact.
- A value close to 1 indicates that the intra-cluster distances are near the maximum possible, signifying poor clustering quality.

The C-Index is particularly useful when comparing the clustering result with an ideal scenario (minimizing intra-cluster distances). Lower values of the C-Index suggest better clustering performance.

- **Akaike and Bayesian Information Criterion.** The Akaike Information Criterion (AIC) and the Bayesian Information Criterion (BIC) [95] are model selection criteria used to evaluate the quality of a clustering model. These criteria are based on the likelihood of the model given the data, but they incorporate penalties to account for model complexity, thus helping to avoid overfitting. The AIC assesses a model's goodness-of-fit while incorporating a penalty score for the number of parameters in order to mitigate the risk of overfitting. In the context of clustering, AIC is used to compare different models (e.g., different numbers of clusters) by balancing the model's fit to the data and its complexity. The formula for AIC is shown in Equation (12):

$$\text{AIC} = 2k - 2 \ln(L) \quad (12)$$

where: k is the number of clusters, L is the likelihood of the model given the data (typically equals to the *inertia*). A lower AIC score indicates a model that provides a good fit to the data while using fewer clusters. However, AIC tends to favor more complex models than the BIC. The BIC, like AIC, evaluates model quality by balancing fit and complexity, but it imposes a stronger penalty for model complexity. BIC is particularly useful when trying to select a model that generalizes well to unseen data. The formula for BIC is shown in Equation (13):

$$\text{BIC} = \ln(n)k - 2 \ln(L) \quad (13)$$

where: n is the number of data points.

BIC includes a logarithmic term, $\ln(n)$, which results in a harsher penalty for additional parameters compared

to AIC, making it more conservative when selecting models. A lower BIC score indicates a better model, with a preference for simpler models that avoid overfitting.

To summarize, AIC is less stringent about penalizing model complexity and may prefer models with more clusters, potentially allowing for more flexible or complex cluster structures, while BIC, being more conservative, tends to select models with fewer clusters, often favoring simpler models that are more likely to generalize well to new data.

Both AIC and BIC can be used to determine the optimal number of clusters in clustering algorithms, by comparing models with different cluster numbers and selecting the one with the lowest AIC or BIC score.

Applying the chosen model identification routine to the above-processed datasets, the results are then compared through the Mean Absolute Percentage Error (MAPE) [96], a statistical index able to express the estimation error as a percentage, defined in Equation (14). Among the defining characteristics and the reason for the choice, it is highlighting the MAPE's intrinsic scale-independence, being suitable to be applied to datasets with varying units and scales, such as the ones concerning the vehicle dynamics and the tyre mechanics (i.e. grip, slip, force, etc) as already presented in similar studies [61], [97], [98].

$$\text{MAPE} = \frac{1}{n} \sum_{i=1}^n \left| \frac{y_i - \hat{y}_i}{y_i} \right|, \quad (14)$$

where y_i represents the measurement and \hat{y}_i is the predicted value for a variable y , both not requiring the assumption of normality [96].

C. HYPERPARAMETERS OPTIMIZATION

In this section, we describe the hyperparameters optimization made for clustering techniques and anomaly detection approaches. Before applying the K-Means and K-Medoids [69], Gaussian Mixture [70], and Hierarchical [71] clustering algorithms on each corner, it was necessary to choose the optimal number of clusters. The authors evaluate their effectiveness in terms of cohesion and separation of clusters by using the Elbow Curve, the Silhouette score, the Calinski-Harabasz, the Davies Bouldin, the Dunn, the C-Index, and the AIC and BIC [95]. Those indices are also used before clustering to choose the optimal number of clusters.

Each index returned a certain value corresponding to the algorithm and the corner to be analyzed, and for each corner and each algorithm, the number of clusters is represented in Table 3.

The next step was to validate the algorithms used with the Calinski-Harabasz, Davies Bouldin, Silhouette, Dun, and C-Index indices. For most indices, the algorithm with the best value is the K-Means for both front – with four clusters – and rear – with six clusters – wheels. The difference in the number of clusters is because the vehicle is rear-wheel drive,

TABLE 3. Number of clusters for each algorithm and each corner once the optimization phase is completed.

| Algorithm | Number of clusters | | | |
|------------------|--------------------|----|----|----|
| | RL | RR | FL | FR |
| K-Means | 6 | 6 | 4 | 4 |
| Gaussian Mixture | 3 | 3 | 4 | 5 |
| Hierarchical | 6 | 6 | 4 | 4 |
| K-Medoids | 5 | 6 | 5 | 5 |

TABLE 4. Hyperparameters for each anomaly detection method once the optimization phase is completed.

| Algorithm | Parameters |
|-----------|---|
| EE | distance: Mahalanobis, contamination: 0.1 |
| LOF | number of neighbors: 5, leaf size: 50 |
| OC-SVM | Kernel: rbf, Nu: 0.5 |
| IF | estimators: 500, max samples: number of items in each cluster |

and therefore the rear wheels are stressed more than the front ones.

Hyperparameters optimization of the anomaly detection algorithms was carried out through graphical representations, identifying the parameters shown in Table 4.

V. RESULTS

In this section, the outcomes of the anomaly detection algorithms applied to each cluster of each dataset are discussed. Results are represented through the curves of the derived variables (i.e., lateral and longitudinal grip) vs. slips. Specifically, some outcomes of the above-described analysis related to front-right (FR) corner are shown in Figure 4 and Figure 5, for the lateral and longitudinal interaction, respectively.

In addition to the anomalies detected by the algorithms, also the ‘NaN’ and infinite values initially identified have been considered as such. The anomalies identified for each corner were corrected by linear interpolation on all the telemetry channels. To assess the performance of the techniques, an identifier was designed to track the parameters of five telemetry datasets—each corresponding to a specific anomaly detection algorithm—as well as the unprocessed telemetry data. This identifier was used to calculate deviations from the target parameters, which were defined at the start of the simulation and represented the characteristics of the tyre being analyzed. The deviations were evaluated under three distinct conditions: pure longitudinal, pure lateral, and combined. The MAPE was employed as the error metric. In Table 5, it can be seen how the identified parameters of the EE technique have the smallest deviation from the target parameters compared to the other algorithm.

TABLE 5. tyre-road interaction deviations of the identified coefficients.

| Condition | Not processed | EE | LOF | OC-SVM | IF |
|-------------------|---------------|-------|-------|--------|-------|
| Pure longitudinal | 2.05% | 0.19% | 0.47% | 0.49% | 0.51% |
| Pure lateral | 1.15% | 0.24% | 0.46% | 0.90% | 0.81% |
| Combined | 1.95% | 0.19% | 0.28% | 1.58% | 1.95% |

TABLE 6. Pure lateral interaction parameters evaluation.

| Algorithm | Slip | | Grip | |
|---------------|---------|---------|---------|---------|
| | Maximum | Minimum | Maximum | Minimum |
| Target | -7.49 | 8.31 | 1.21 | -1.22 |
| Not processed | 4.41% | 4.2% | 3.71% | 3.71% |
| EE | 0.63% | 0.60% | 0.25% | 0.25% |
| LOF | 1.89% | 1.80% | 1.10% | 1.10% |
| IF | 1.26% | 1.20% | 0.66% | 0.66% |
| OC-SVM | 0.01% | 0.01% | 0.01% | 0.07% |

TABLE 7. Pure longitudinal interaction parameters evaluation.

| Algorithm | Slip | | Grip | |
|---------------|---------|---------|---------|---------|
| | Maximum | Minimum | Maximum | Minimum |
| Target | 10.65 | -10.65 | 1.45 | -1.44 |
| Not processed | 3.76% | 1.90% | 2.94% | 2.94% |
| EE | 1.88% | 1.90% | 0.30% | 0.30% |
| LOF | 3.75% | 3.79% | 0.69% | 0.69% |
| IF | 0.01% | 0.01% | 0.21% | 0.21% |
| OC-SVM | 1.88% | 1.90% | 0.14% | 0.14% |

To evaluate the physical characteristics of tyre behavior, the previously identified parameters were re-simulated under pure lateral and pure longitudinal conditions to obtain the lateral and longitudinal grip curves as a function of the slips.

Some fundamental points were taken into consideration for each curve: the stiffness value, which identifies the angle of inclination of the linear section, the maximum values of the lateral and longitudinal grip, and the slip values at the maximum and minimum values of the lateral and longitudinal grip (see Figs. 6 and 7).

To analyze the physical phenomenon, the deviations of the characteristic points of the simulated curves from the target were assessed using the MAPE metric. As shown in Table 6, under pure lateral conditions, the curve most closely matching the target parameters is the one simulated using the telemetry parameters corrected with the OC-SVM method. Instead, as shown in Table 7, under pure longitudinal conditions, the curve that best matches the target parameters varies depending on the analysis criteria. When examining the maximum and minimum longitudinal grip values, the closest match is achieved using the parameters determined

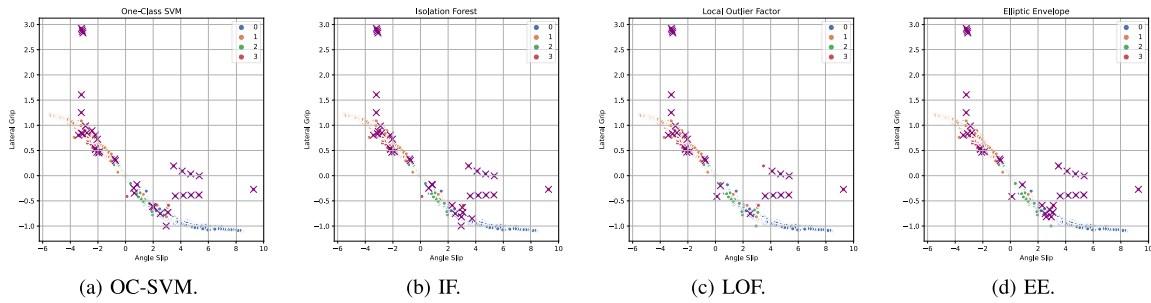


FIGURE 4. Anomaly detection by ML algorithms (lateral interaction).

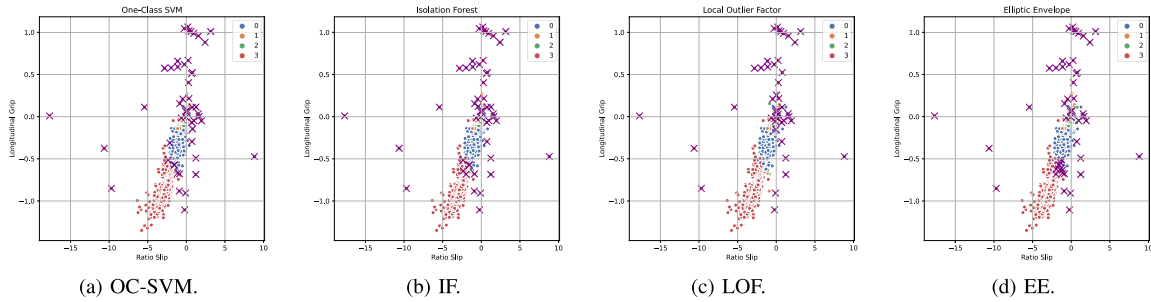


FIGURE 5. Anomaly detection by ML algorithms (longitudinal interaction).

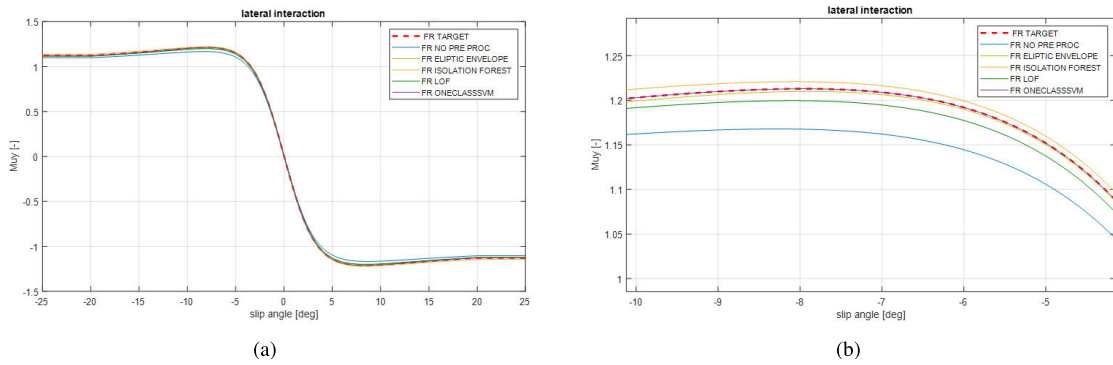


FIGURE 6. Pure lateral interaction.

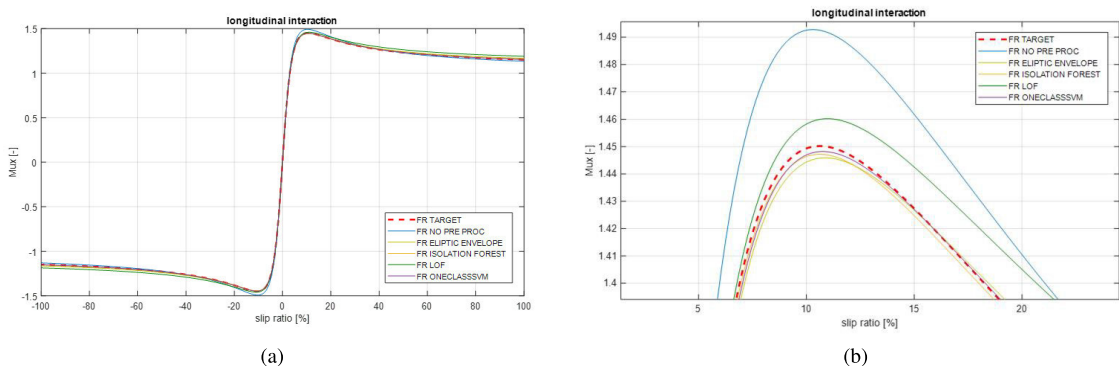


FIGURE 7. Pure longitudinal interaction.

from telemetry corrected with the OC-SVM. However, when analyzing stiffness and slip values at the maximum and

minimum, the curve most closely aligns with the target parameters when using the telemetry corrected with the IF.

TABLE 8. Stiffness evaluation.

| Algorithm | Stiffness | |
|---------------|-----------|--------------|
| | Lateral | Longitudinal |
| Target | -0.38 | 0.43 |
| Not processed | 3.21% | 1.92% |
| EE | 0.08% | 0.77% |
| LOF | 0.93% | 0.37% |
| IF | 1.62% | 0.35% |
| OC-SVM | 0.01% | 1.09% |

Finally, the majority of the state-of-the-art approach focus on classifying tyre tread wear [43], which presents challenges due to the difficulty in defining an appropriate number of classes. Relying on predefined classes can also limit the effectiveness of the detection of tyre wear since it struggles to capture the complex and nonlinear dynamics of tyre-road interactions, which significantly influence tire consumption. In turn, the proposed approach first applies clustering algorithms to group samples with similar behaviors without establishing a previous number of classes, followed by anomaly detection techniques to identify and analyze tire behaviors that deviate from the norm.

VI. CONCLUSION

This paper has comprehensively analyzed the challenges of observing and understanding multi-dimensional tyre-related data. The authors have highlighted the critical importance of data quality as a necessary starting point for the tyre's model calibration, shedding light on the complexities involved in defining outliers within both univariate and multivariate datasets and emphasizing the need for a scientific investigation of the approaches able to identify and mitigate anomalies.

Following the data pre-processing phase, aimed at removing duplicated data and assuring temporal continuity of all the acquired signals, different clustering approaches are discussed and applied to group observations based on tyre-related features such as maximum friction coefficient and stiffness variations. Four different clustering algorithms (i.e., K-Means, K-Medoids, Gaussian Mixture, and Hierarchical) were chosen and compared. To identify anomalies, four unsupervised algorithms (i.e., One-Class Support Vector Machine (SVM or OC-SVM), Isolation Forest (IF), Local Outlier Factor (LOF) and Elliptic Envelope (EE)) have been employed.

Results have shown that applying K-Means to identify similar conditions of forces is the most efficient way to differentiate the anomalies identified in the diverse conditions of grip and, therefore, the behavior of the tyre. Following the clustering phase, where the K-Means method was preferred, the results showed that all detection algorithms of anomalies employed correctly identify anomalous observations. It should be highlighted that the corrections carried out through linear interpolation on anomalies identified have

been applied to all telemetry channels and are fundamental in bringing these values back to the "normal observability range". Hence, our methodology improves the identification of anomalies related to tyre-road interaction phenomena by reducing the noise introduced by sensor measurements and the misestimate of vehicle-tyre parameters. Furthermore, the proposed approach identifies anomalies without establishing a previous number of classes. This demonstrates the efficiency of identifying tyre characteristics using a tyre reference model for validation. By utilizing and comparing different clustering approaches, we have been able to focus subsequent anomaly detection studies on a subset of data related to tyre behavior that better describes the expected normality.

To objectively compare the data processing results, the authors have employed the resulting "corrected" datasets for the calibration of the tyre model, comparing the deviations in terms of fundamental tyre-related quantities towards the previously identified tyre model, already validated in offline and online scenarios. In this case, the Elliptic Envelope technique resulted to be the best anomaly detection technique for the grip coefficient evaluation, whereas the One-Class Support Vector Machine technique shows lower deviations for the stiffness evaluation in both longitudinal and lateral directions.

Some limitations pertain to the proposed analysis. One challenge concerns the complexity of identifying normal behavior and choosing suitable thresholds that require a large amount of data. Sensor measurement uncertainty can further affect the effectiveness of the proposed approach. To mitigate these limitations, the authors underline the relevance of collecting and processing robust data during the proposed analysis.

Future work should focus on refining the methodologies for outlier detection and data quality assessment and expanding the range of operating conditions under which tyre behavior is analyzed. By continuing to address the challenges outlined in this paper, researchers and practitioners can further improve the fidelity of tyre-road interaction models. This, in turn, will facilitate the development of advanced driver-assistance systems and autonomous vehicles, ensuring that the safety and performance of road transportation continue to progress in the years to come.

ACKNOWLEDGMENT

The authors would like to thank Giancarlo Aprea and Luisana Coppola for their support in integrating the described algorithm within these paths.

REFERENCES

- [1] T. Erol, A. F. Mendi, and D. Dogan, "Digital transformation revolution with digital twin technology," in *Proc. 4th Int. Symp. Multidisciplinary Stud. Innov. Technol. (ISMSIT)*, Oct. 2020, pp. 1–7.
- [2] D. M. Botín-Sanabria, A.-S. Mihaita, R. E. Peimbert-García, M. A. Ramírez-Moreno, R. A. Ramírez-Mendoza, and J. D. J. Lozoya-Santos, "Digital twin technology challenges and applications: A comprehensive review," *Remote Sens.*, vol. 14, no. 6, p. 1335, Mar. 2022.

- [3] S. Yang, Y. Chen, R. Shi, R. Wang, Y. Cao, and J. Lu, "A survey of intelligent tires for tire-road interaction recognition toward autonomous vehicles," *IEEE Trans. Intell. Vehicles*, vol. 7, no. 3, pp. 520–532, Sep. 2022.
- [4] G. Bhatti, H. Mohan, and R. Raja Singh, "Towards the future of smart electric vehicles: Digital twin technology," *Renew. Sustain. Energy Rev.*, vol. 141, May 2021, Art. no. 110801.
- [5] J. Wu, X. Wang, Y. Dang, and Z. Lv, "Digital twins and artificial intelligence in transportation infrastructure: Classification, application, and future research directions," *Comput. Electr. Eng.*, vol. 101, Jul. 2022, Art. no. 107983.
- [6] D. Fischer and R. Isermann, "Mechatronic semi-active and active vehicle suspensions," *Control Eng. Pract.*, vol. 12, no. 11, pp. 1353–1367, Nov. 2004.
- [7] M. Sharifzadeh, A. Senatore, A. Farnam, A. Akbari, and F. Timpone, "A real-time approach to robust identification of tyre-road friction characteristics on mixed- μ roads," *Vehicle Syst. Dyn.*, vol. 57, no. 9, pp. 1338–1362, Sep. 2019.
- [8] A. Sakhnevych, V. M. Arricale, M. Bruschetta, A. Censi, E. Mion, E. Picotti, and E. Frazzoli, "Investigation on the model-based control performance in vehicle safety critical scenarios with varying tyre limits," *Sensors*, vol. 21, no. 16, p. 5372, Aug. 2021.
- [9] F. van Wyk, Y. Wang, A. Khojandi, and N. Masoud, "Real-time sensor anomaly detection and identification in automated vehicles," *IEEE Trans. Intell. Transp. Syst.*, vol. 21, no. 3, pp. 1264–1276, Mar. 2020.
- [10] Y. Wang, N. Masoud, and A. Khojandi, "Real-time sensor anomaly detection and recovery in connected automated vehicle sensors," *IEEE Trans. Intell. Transp. Syst.*, vol. 22, no. 3, pp. 1411–1421, Mar. 2021.
- [11] M. Abboush, C. Knieke, and A. Rausch, "GRU-based denoising autoencoder for detection and clustering of unknown single and concurrent faults during system integration testing of automotive software systems," *Sensors*, vol. 23, no. 14, p. 6606, Jul. 2023.
- [12] S. Verma, S. Parkinson, and S. Khan, "Detecting abnormal vehicle behavior: A clustering-based approach," in *Deception in Autonomous Transport Systems: Threats, Impacts and Mitigation Policies*. Cham, Switzerland: Springer, 2024, pp. 99–110.
- [13] Y. Wang, J. Hu, F. Wang, H. Dong, Y. Yan, Y. Ren, C. Zhou, and G. Yin, "Tire road friction coefficient estimation: Review and research perspectives," *Chin. J. Mech. Eng.*, vol. 35, no. 1, p. 6, Dec. 2022.
- [14] L. Hermansdorfer, R. Trauth, J. Betz, and M. Lienkamp, "End-to-end neural network for vehicle dynamics modeling," in *Proc. 6th IEEE Congr. Inf. Sci. Technol. (CiSt)*, Jun. 2020, pp. 407–412.
- [15] D. Lee, J.-C. Kim, M. Kim, and H. Lee, "Intelligent tire sensor-based real-time road surface classification using an artificial neural network," *Sensors*, vol. 21, no. 9, p. 3233, May 2021.
- [16] A. Sakhnevych and A. Genovese, "Tyre wear model: A fusion of rubber viscoelasticity, road roughness, and thermodynamic state," *Wear*, vols. 542–543, Apr. 2024, Art. no. 205291.
- [17] F. Braghin, M. Brusarosco, F. Cheli, A. Cigada, S. Manzoni, and F. Mancosu, "Measurement of contact forces and patch features by means of accelerometers fixed inside the tire to improve future car active control," *Vehicle Syst. Dyn.*, vol. 44, no. sup1, pp. 3–13, Jan. 2006.
- [18] F. Coppo, G. Pepe, N. Roveri, and A. Carcaterra, "A multisensing setup for the intelligent tire monitoring," *Sensors*, vol. 17, no. 3, p. 576, Mar. 2017.
- [19] T. Dózsa, J. Radó, J. Volk, Á. Kisari, A. Soumelidis, and P. Kovács, "Road abnormality detection using piezoresistive force sensors and adaptive signal models," *IEEE Trans. Instrum. Meas.*, vol. 71, pp. 1–11, 2022.
- [20] Z. Wang, Y. Wu, and Q. Niu, "Multi-sensor fusion in automated driving: A survey," *IEEE Access*, vol. 8, pp. 2847–2868, 2020.
- [21] E. Blasch, T. Pham, C.-Y. Chong, W. Koch, H. Leung, D. Braines, and T. Abdelzaher, "Machine learning/artificial intelligence for sensor data fusion—opportunities and challenges," *IEEE Aerosp. Electron. Syst. Mag.*, vol. 36, no. 7, pp. 80–93, Jul. 2021.
- [22] M. Tanelli, L. Piroddi, and S. M. Savaresi, "Real-time identification of tire-road friction conditions," *IET Control Theory Appl.*, vol. 3, no. 7, pp. 891–906, 2009.
- [23] N. Silva, V. Shah, J. Soares, and H. Rodrigues, "Road anomalies detection system evaluation," *Sensors*, vol. 18, no. 7, p. 1984, Jun. 2018.
- [24] H. M. Ngwangwa, P. S. Heyns, H. G. A. Breytenbach, and P. S. Els, "Reconstruction of road defects and road roughness classification using artificial neural networks simulation and vehicle dynamic responses: Application to experimental data," *J. Terramechanics*, vol. 53, pp. 1–18, Jun. 2014.
- [25] D. Luo, J. Lu, and G. Guo, "Road anomaly detection through deep learning approaches," *IEEE Access*, vol. 8, pp. 117390–117404, 2020.
- [26] C. Gorges, K. Öztürk, and R. Liebich, "Impact detection using a machine learning approach and experimental road roughness classification," *Mech. Syst. Signal Process.*, vol. 117, pp. 738–756, Feb. 2019.
- [27] N. Silva, J. Soares, V. Shah, M. Y. Santos, and H. Rodrigues, "Anomaly detection in roads with a data mining approach," *Proc. Comput. Sci.*, vol. 121, pp. 415–422, Jan. 2017.
- [28] S. Sattar, S. Li, and M. Chapman, "Developing a near real-time road surface anomaly detection approach for road surface monitoring," *Measurement*, vol. 185, Nov. 2021, Art. no. 109990.
- [29] S. Liu, L. Liu, J. Tang, B. Yu, Y. Wang, and W. Shi, "Edge computing for autonomous driving: Opportunities and challenges," *Proc. IEEE*, vol. 107, no. 8, pp. 1697–1716, Aug. 2019.
- [30] D. T. Kanapram, P. Marin-Plaza, L. Marcenaro, D. Martin, A. de la Escalera, and C. Regazzoni, "Self-awareness in intelligent vehicles: Feature based dynamic Bayesian models for abnormality detection," *Robot. Auto. Syst.*, vol. 134, Dec. 2020, Art. no. 103652.
- [31] M. A. Quraan, "Efficient and effective anomaly detection in autonomous vehicles: A combination of gradient boosting and ANFIS algorithms," *Int. J. Fuzzy Syst.*, vol. 2024, pp. 1–17, Sep. 2024.
- [32] H. Pacejka, *Tire and Vehicle Dynamics*. Amsterdam, The Netherlands: Elsevier, 2005.
- [33] S. Mihajlovic, U. Kutscher, B. Wies, and J. Wallaschek, "Methods for experimental investigations on tyre-road-grip at arbitrary roads," in *Proc. 5th Int. Conf. ESAR*, May 2013, pp. 234–249.
- [34] L. R. Ray, "Nonlinear state and tire force estimation for advanced vehicle control," *IEEE Trans. Control Syst. Technol.*, vol. 3, no. 1, pp. 117–124, Mar. 1995.
- [35] A. Sakhnevych, "Multiphysical MF-based tyre modelling and parametrisation for vehicle setup and control strategies optimisation," *Vehicle Syst. Dyn.*, vol. 60, no. 10, pp. 3462–3483, Oct. 2022.
- [36] C. M. Greve, K. Hara, R. S. Martin, D. Q. Eckhardt, and J. W. Koo, "A data-driven approach to model calibration for nonlinear dynamical systems," *J. Appl. Phys.*, vol. 125, no. 24, Jun. 2019, Art. no. 244901.
- [37] L. Bürger and F. Naets, "High fidelity nonlinear finite element tire modeling for dynamic analysis: Total Lagrangian formulation in rolling contact," *J. Sound Vib.*, vol. 571, Feb. 2024, Art. no. 118098.
- [38] F. Farroni, "Trick-tire/road interaction characterization & knowledge—A tool for the evaluation of tire and vehicle performances in outdoor test sessions," *Mech. Syst. Signal Process.*, vol. 72, pp. 808–831, May 2016.
- [39] P. Faithfull, R. Ball, and R. Jones, "An investigation into the use of hardware-in-the-loop simulation with a scaled physical prototype as an aid to design," *J. Eng. Des.*, vol. 12, no. 3, pp. 231–243, Sep. 2001.
- [40] K. Li, J. Cao, and F. Yu, "Nonlinear tire-road friction control based on tire model parameter identification," *Int. J. Automot. Technol.*, vol. 13, no. 7, pp. 1077–1088, Dec. 2012.
- [41] N. Xu, J. Zhou, B. H. G. Barbosa, H. Askari, and A. Khajepour, "A soft sensor for estimating tire cornering properties for intelligent tires," *IEEE Trans. Syst., Man, Cybern., Syst.*, vol. 53, no. 10, pp. 6056–6066, Oct. 2023.
- [42] B. H. G. Barbosa, N. Xu, H. Askari, and A. Khajepour, "Lateral force prediction using Gaussian process regression for intelligent tire systems," *IEEE Trans. Syst., Man, Cybern., Syst.*, vol. 52, no. 8, pp. 5332–5343, Aug. 2022.
- [43] J.-Y. Han, J.-H. Kwon, S. Lee, K.-C. Lee, and H.-J. Kim, "Experimental evaluation of tire tread wear detection using machine learning in real-road driving conditions," *IEEE Access*, vol. 11, pp. 32996–33004, 2023.
- [44] L. Gutiérrez-Gómez, F. Petry, and D. Khadraoui, "A comparison framework of machine learning algorithms for mixed-type variables datasets: A case study on tire-performances prediction," *IEEE Access*, vol. 8, pp. 214902–214914, 2020.
- [45] L. C. Sousa and H. V. H. Ayala, "Nonlinear tire model approximation using machine learning for efficient model predictive control," *IEEE Access*, vol. 10, pp. 107549–107562, 2022.
- [46] E. M. Kasprzak and D. Gentz, "The formula SAE tire test consortium-tire testing and data handling," SAE Tech. Paper 2006-01-3606, 2006.
- [47] R. Rugsaj and C. Suvanjumrat, "Mechanical characteristics of airless tyre by laboratory testing," *IOP Conf. Ser., Mater. Sci. Eng.*, vol. 773, no. 1, Feb. 2020, Art. no. 012037.
- [48] J. L. Sommerfeld and R. A. Meyer, "Correlation and accuracy of a wheel force transducer as developed and tested on a flat-trac@ tire test system," SAE Tech. Paper 1999-01-0938, 1999.

- [49] M. Furlan, H. Olsson, M. Gladstone, and G. Mavros, "Effects of different tire operating conditions on transient lateral tire response," *Tire Sci. Technol.*, vol. 49, no. 1, pp. 19–38, Jan. 2021.
- [50] A. Albinsson, F. Bruzelius, B. Jacobson, and E. Bakker, "Evaluation of vehicle-based tyre testing methods," *Proc. Inst. Mech. Eng., D, J. Automobile Eng.*, vol. 233, no. 1, pp. 4–17, Jan. 2019.
- [51] K. D. Bird and J. F. Martin, "The calspan tire research facility: Design, development, and initial test results," *SAE Trans.*, vol. 82, pp. 2012–2027, Feb. 1973.
- [52] M. G. Pottinger, "The flat-trac II® machine, the state-of-the-art in tire force and moment measurement," *Tire Sci. Technol.*, vol. 20, no. 3, pp. 132–153, Jul. 1992.
- [53] P. Els, "Wheel force transducer research and development," Pretoria Univ., Pretoria, South Africa, Tech. Rep. 0704-0188, 2012.
- [54] F. Cheli, F. Braghin, M. Brusarosco, F. Mancosu, and E. Sabbioni, "Design and testing of an innovative measurement device for tyre-road contact forces," *Mech. Syst. Signal Process.*, vol. 25, no. 6, pp. 1956–1972, Aug. 2011.
- [55] S. Cheng, L. Li, B. Yan, C. Liu, X. Wang, and J. Fang, "Simultaneous estimation of tire side-slip angle and lateral tire force for vehicle lateral stability control," *Mech. Syst. Signal Process.*, vol. 132, pp. 168–182, Oct. 2019.
- [56] T. A. Wenzel, K. J. Burnham, M. V. Blundell, and R. A. Williams, "Dual extended Kalman filter for vehicle state and parameter estimation," *Vehicle Syst. Dyn.*, vol. 44, no. 2, pp. 153–171, Feb. 2006.
- [57] A. Kheiralla, A. Yahya, M. Z. Bardaie, and W. Wan Ismail, "Design, development and calibration of a drive wheel torque transducer for an agricultural tractor," *Pertanika J. Sci. Technol.*, vol. 11, no. 2, pp. 311–324, 2003.
- [58] F. Braghin, F. Cheli, and E. Sabbioni, "Identification of tire model parameters through full vehicle experimental tests," *J. Dyn. Meas., Control*, vol. 133, no. 3, pp. 031006-1–031006-11, May 2011.
- [59] L. Merkx, "Overturning moment analysis using the flat plank tyre tester," *DCT Rapporten*, vol. 2004, pp. 1–14, Jan. 2004.
- [60] H. C. Sonderegger, R. Calderara, M. Giorgetta, D. Barberis, and M. Caprez, "Force sensor systems especially for determining dynamically the axle load, speed, wheelbase and gross weight of vehicles," U.S. Patent 5 265 481, Nov. 30, 1993.
- [61] M. Barbaro, A. Genovese, F. Timpone, and A. Sakhnevych, "Extension of the multiphysical magic formula tire model for ride comfort applications," *Nonlinear Dyn.*, vol. 112, no. 6, pp. 4183–4208, Mar. 2024.
- [62] P. Lugner, H. Pacejka, and M. Plöchl, "Recent advances in tyre models and testing procedures," *Vehicle Syst. Dyn.*, vol. 43, nos. 6–7, pp. 413–426, Jun. 2005.
- [63] F. Farroni, M. Russo, R. Russo, and F. Timpone, "Tyre-road interaction: Experimental investigations about the friction coefficient dependence on contact pressure, road roughness, slide velocity and temperature," *Eng. Syst. Design Anal.*, vol. 44878, pp. 521–529, Jul. 2012.
- [64] Kistler Group. *Non-Contact Optical Sensors Correvit S-Motion*. Accessed: Jan. 13, 2024. [Online]. Available: <https://kistler.cdn.celum.cloud/SAPCommerceDownloadoriginal/003-395e.pdf>
- [65] Mazda. *Abs Sensor Wire*. Accessed: Jan. 13, 2024. [Online]. Available: <https://www.realmazdaparts.com/oem-parts/mazda-abs-sensor-wire-c23567sh1c?c=bD000CZuPVNIYXJJaCBSZXN1bHRZ>
- [66] H. B. Pacejka and I. J. M. Besselink, "Magic formula tyre model with transient properties," *Vehicle Syst. Dyn.*, vol. 27, no. 1, pp. 234–249, 1996.
- [67] E. Kreyszig, H. Kreyszig, and E. J. Norminton, *Advanced Engineering Mathematics*. Hoboken, NJ, USA: Wiley, 2011.
- [68] A. E. Ezugwu, A. M. Ikotun, O. O. Oyelade, L. Abualigah, J. O. Agushaka, C. I. Eke, and A. A. Akinyelu, "A comprehensive survey of clustering algorithms: State-of-the-art machine learning applications, taxonomy, challenges, and future research prospects," *Eng. Appl. Artif. Intell.*, vol. 110, Apr. 2022, Art. no. 104743.
- [69] T. Velmurugan and T. Santhanam, "Computational complexity between K-means and K-medoids clustering algorithms for normal and uniform distributions of data points," *J. Comput. Sci.*, vol. 6, no. 3, pp. 363–368, Mar. 2010.
- [70] G. J. McLachlan and S. Rathnayake, "On the number of components in a Gaussian mixture model," *WIREs Data Mining Knowl. Discovery*, vol. 4, no. 5, pp. 341–355, Sep. 2014.
- [71] M. L. Zepeda-Mendoza and O. Resendis-Antonio, *Hierarchical Agglomerative Clustering*. New York, NY, USA: Springer, 2013, pp. 886–887, doi: 10.1007/978-1-4419-9863-7_1371.
- [72] A. Paleyes, R.-G. Urma, and N. D. Lawrence, "Challenges in deploying machine learning: A survey of case studies," *ACM Comput. Surv.*, vol. 55, no. 6, pp. 1–29, Dec. 2022.
- [73] A. A. Alwan, M. A. Ciupala, A. J. Brimicombe, S. A. Ghorashi, A. Baravalle, and P. Falcarin, "Data quality challenges in large-scale cyber-physical systems: A systematic review," *Inf. Syst.*, vol. 105, Mar. 2022, Art. no. 101951.
- [74] G. Pang, C. Shen, L. Cao, and A. V. D. Hengel, "Deep learning for anomaly detection: A review," *ACM Comput. Surv.*, vol. 54, no. 2, pp. 1–10, Mar. 2021.
- [75] M. Carletti, M. Terzi, and G. A. Susto, "Interpretable anomaly detection with DIFFI: Depth-based feature importance of isolation forest," *Eng. Appl. Artif. Intell.*, vol. 119, Mar. 2023, Art. no. 105730.
- [76] A. Blázquez-García, A. Conde, U. Mori, and J. A. Lozano, "A review on outlier/anomaly detection in time series data," *ACM Comput. Surv.*, vol. 54, no. 3, pp. 1–33, Apr. 2021.
- [77] Y. Regaya, F. Fadli, and A. Amira, "Point-denoise: Unsupervised outlier detection for 3D point clouds enhancement," *Multimedia Tools Appl.*, vol. 80, no. 18, pp. 28161–28177, Jul. 2021.
- [78] B. Ray, S. Ghosh, S. Ahmed, R. Sarkar, and M. Nasipuri, "Outlier detection using an ensemble of clustering algorithms," *Multimedia Tools Appl.*, vol. 81, no. 2, pp. 2681–2709, Jan. 2022.
- [79] B. Schölkopf, R. Williamson, A. Smola, J. Shawe-Taylor, and J. Platt, "Support vector method for novelty detection," in *Advances in Neural Information Processing Systems*. Cambridge, MA, USA: MIT Press, Jun. 2000, pp. 582–588.
- [80] A. Bounsiar and M. G. Madden, "Kernels for one-class support vector machines," in *Proc. Int. Conf. Inf. Sci. Appl. (ICISA)*, May 2014, pp. 1–4.
- [81] V. N. Vapnik, *The Nature of Statistical Learning Theory*. Cham, Switzerland: Springer, 2000.
- [82] F. T. Liu, K. M. Ting, and Z. Zhou, "Isolation forest," in *Proc. 8th IEEE Int. Conf. Data Mining*, Dec. 2008, pp. 413–422.
- [83] F. T. Liu, K. M. Ting, and Z. Zhou, "Isolation-based anomaly detection," *ACM Trans. Knowl. Discov. Data*, vol. 6, no. 1, pp. 1–39, Mar. 2012.
- [84] M. M. Breunig, H.-P. Kriegel, R. T. Ng, and J. Sander, "LOF: Identifying density-based local outliers," *ACM SIGMOD Rec.*, vol. 29, no. 2, pp. 93–104, Jun. 2000.
- [85] Y. Chen, S. Wang, Q. Zhao, and G. Sun, "Detection of multivariate geochemical anomalies using the bat-optimized isolation forest and bat-optimized elliptic envelope models," *J. Earth Sci.*, vol. 32, no. 2, pp. 415–426, Apr. 2021.
- [86] B. Hoyle, M. M. Rau, K. Paech, C. Bonnett, S. Seitz, and J. Weller, "Anomaly detection for machine learning redshifts applied to SDSS galaxies," *Monthly Notices Roy. Astronomical Soc.*, vol. 452, no. 4, pp. 4183–4194, Aug. 2015.
- [87] J.-O. Palacio-Niño and F. Berzal, "Evaluation metrics for unsupervised learning algorithms," 2019, *arXiv:1905.05667*.
- [88] M. Charrad, N. Ghazzali, V. Boiteau, and A. Niknafs. (2012). *NbClust Package. An Examination of Indices for Determining the Number of Clusters*. [Online]. Available: <http://cran.r-project.org/>
- [89] R. L. Thorndike, "Who belongs in the family?" *Psychometrika*, vol. 18, no. 4, pp. 267–276, Dec. 1953.
- [90] P. J. Rousseeuw, "Silhouettes: A graphical aid to the interpretation and validation of cluster analysis," *J. Comput. Appl. Math.*, vol. 20, pp. 53–65, Nov. 1987.
- [91] T. Calinski and J. Harabasz, "A dendrite method for cluster analysis," *Commun. Statist. - Simul. Comput.*, vol. 3, no. 1, pp. 1–27, 1974.
- [92] D. L. Davies and D. W. Bouldin, "A cluster separation measure," *IEEE Trans. Pattern Anal. Mach. Intell.*, vols. PAMI-1, no. 2, pp. 224–227, Apr. 1979.
- [93] J. C. Dunn, "Well-separated clusters and optimal fuzzy partitions," *J. Cybern.*, vol. 4, no. 1, pp. 95–104, Jan. 1974.
- [94] L. J. Hubert and J. R. Levin, "A general statistical framework for assessing categorical clustering in free recall," *Psychol. Bull.*, vol. 83, no. 6, pp. 1072–1080, 1976.
- [95] A. Chakrabarti and J. K. Ghosh, "AIC, BIC and recent advances in model selection," in *Philosophy of Statistics* (Handbook of the Philosophy of Science), vol. 7, P. S. Bandyopadhyay and M. R. Forster, Eds., Amsterdam, The Netherlands: North-Holland, 2011, pp. 583–605.
- [96] C. Tofallis, "A better measure of relative prediction accuracy for model selection and model estimation," *J. Oper. Res. Soc.*, vol. 66, no. 8, pp. 1352–1362, Aug. 2015.

- [97] Z. Ma, X. Ji, Y. Zhang, and J. Yang, "State estimation in roll dynamics for commercial vehicles," *Vehicle Syst. Dyn.*, vol. 55, no. 3, pp. 313–337, Mar. 2017.
- [98] M. Greiner, H.-J. Unrau, and F. Gauterin, "A model for prediction of the transient rolling resistance of tyres based on inner-liner temperatures," *Vehicle Syst. Dyn.*, vol. 56, no. 1, pp. 78–94, Jan. 2018.



ALEKSANDR SAKHNEVYCH is an Assistant Professor of applied mechanics and vehicle dynamics with the Department of Industrial Engineering, Università degli Studi di Napoli Federico II, and a CTO of MegaRide applied vehicle research. With a keen focus on tyre-road interaction, his research activities are closely related to the understanding and modeling of the tribological aspects with the specific aim of bridging the gap between indoor/outdoor vehicle/tire testing and the reproduction of the system under study within the real-time simulation environment. His innovative work aims to enhance safety and performance in automotive engineering, contributing significantly to the field through both teaching and pioneering research.



NICOLA PASQUINO (Senior Member, IEEE) was born in Naples, Italy, in 1973. He received the M.Sc. degree (magna cum laude) in electronics engineering and the Ph.D. degree in information engineering from the Università degli Studi di Napoli Federico II, Naples, in 1998 and 2002, respectively.

He was a Fulbright Scholar with the University of Pennsylvania, Philadelphia, PA, USA, from 2000 to 2001. He is currently a Professor of electrical and electronic measurements with the Dipartimento di Ingegneria Elettrica e della Tecnologie dell'Informazione, Università degli Studi di Napoli Federico II, where he is also the Chief Scientist with the Electromagnetic Compatibility Laboratory. His research interests include measurements of human exposure to high-frequency electromagnetic fields and the application of machine learning methodologies to measurement data analysis.

Prof. Pasquino is a member of TC37 of IEEE. He is the Chair of the TC106 "Human Exposure to Electromagnetic Fields" of Italian Electrotechnical Committee (CEI). He is also the Chair of the Committee on "Human Exposure to Electromagnetic Fields" within the Engineering Register of Naples. He is a member of the editorial board of the *Measurement Science Review*. He serves as an Editor for *Journal of Electrical and Computer Engineering* and a Section Editor for *Acta IMEKO*.



GIANCARLO SPERLI (Member, IEEE) received the Ph.D. degree in information technology and electrical engineering from the Università degli Studi di Napoli Federico II. He defended his Ph.D. thesis: "Multimedia Social Networks." He is an Associate Professor with the Department of Electrical Engineering and Information Technology, Università degli Studi di Napoli Federico II. He is a member of the Pattern analysis and Intelligent Computation for mUltimedia Systems (PICUS) departmental research groups. He has authored about 131 publications in international journals, conference proceedings, and book chapters. His main research interests include cybersecurity, semantic analysis of multimedia data, and social networks analysis. He served as a guest editor for different special issues on international journals.

...